Dynamics for the Assembly of Pyrene−γ-Cyclodextrin Host−Guest Complexes

Andria S. M. Dyck, Ursula Kisiel, and Cornelia Bohne*

Department of Chemistry, University of Victoria, P.O. Box 3065, Victoria, B.C., Canada V8W 3V6

Received: June 2, 2003; In Final Form: August 5, 2003

Pyrene and γ-cyclodextrin (γ-CD) form complexes with 1:1, 1:2, and 2:2 (pyrene/CD) stoichiometries. The complexation dynamics was studied using stopped flow. The dynamics for the higher-order complexes (1:2 and 2:2) occurs in the millisecond time domain, which contrasts with the much faster dynamics for the 1:1 complex. When pyrene is mixed with γ-CD, a transient enhancement of the concentration for the 2:2 complex was observed between 0.2 and 1 s, which at longer times leads to the formation of the 1:2 complex. This enhancement of the nonthermodynamic product is an example of the kinetic formation of a host−guest complex, and these types of processes may be explored to build self-assemblies under kinetic control.

Introduction

Supramolecular chemistry is an expanding field where many different structural motifs have been explored.[1−3] The principal objective of supramolecular chemistry is to perform new functions such as catalysis or transport that are not available for the individual components of these structures. In contrast to molecular chemistry, supramolecular architectures are always reversible systems. This dynamic nature is frequently essential for supramolecular function to be expressed. Dynamic processes are also essential in self-assembly where frequent reversible error-correction processes are required on the path to the final self-assembly.[4−6]

The field of supramolecular chemistry has been driven by the synthesis of elaborate and sophisticated structures. The structures of supramolecular systems are routinely established by NMR or X-ray crystallography, and the thermodynamics is frequently reported. Kinetic measurements have been less prevalent, in part, because many of the processes involved occur on fast time scales (nano- to microseconds) and require fast kinetic techniques.[7] Kinetic information is unavailable from thermodynamic measurements. For this reason, to exploit the potential of supramolecular systems fully it is necessary to characterize the structural, thermodynamic, and dynamic properties of each system.

Self-assemblies are supramolecular architectures where structures with well-defined stoichiometries are formed spontaneously.[1,2,5] Most self-assemblies are formed under thermodynamic control. The type of structure and topology obtained for each self-assembly can be controlled by changing the concentration ratio of molecular building blocks. A larger number of structures would become available if one could form assemblies under kinetic control.

In this work, we describe the dynamics for the formation of the complexes between pyrene and γ-cyclodextrin (γ-CD), where one of the complexes is enhanced under kinetic control. This work exemplifies with a very simple host−guest complex the dynamic processes that will be required to explore the kinetic control of self-assemblies.

* Corresponding author. E-mail: bohne@uvic.ca. http://www.foto.chem.uvic.ca/. Phone: 250-721-7151. Fax: 250-721-7147.

Experimental Section

Materials and Sample Preparation. Pyrene (Polysciences Inc. or Aldrich, 99%) was recrystalized once from 95% ethanol. Its purity was checked by measuring the fluorescence decay in water, where a monoexponential decay was observed for pure samples. γ-CD (lots E 8056 and F 8025-12) was a generous gift from Cerestar and was used without further purification. Sodium iodide (BDH or Aldrich, ≥99%), tetrabutylammonium iodide (Sigma-Aldrich), methanol (ACP, spectrograde), acetonitrile (CALEDON, HPLC grade, ≥99.8%), sodium hydroxide (ACP, ≥97%), and D_2O (CDN Isotopes) were used as received. Deionized water (SYBRON Barnstead system) was used for all solutions.

Aqueous pyrene solutions (0.25−1 μM) were prepared by injecting small amounts of a pyrene methanolic solution (1.5−3.5 mM) into water and stirring the solution overnight. Two different methods were employed to prepare the pyrene−γ-CD solutions: (i) the pyrene methanol solution was injected directly into an aqueous solution in which the desired amount of γ-CD had been dissolved, or (ii) the appropriate amount of γ-CD was dissolved in the aqueous pyrene stock solution. The samples were stirred for at least 12 h. All measurements were performed in aerated solutions. The second method was employed for the preparation of the samples in D_2O.

Instrumentation. UV−vis absorption spectra were measured with a Varian Cary 5 spectrophotometer at room temperature. A PTI QM2 fluorimeter was employed for steady-state fluorescence measurements (20.0 ± 0.2 °C). The excitation and emission slits were set such that the bandpass for each was 3 nm. The solutions were excited at 331 nm, and the emission was collected between 345 and 550 nm. Excitation spectra were collected by monitoring the emission at 383 or 473 nm for the monomer and excimer fluorescence, respectively. All pyrene spectra were corrected by subtracting the collected spectra containing all components except pyrene. Time-resolved fluorescence decays were measured with a PTI LS-1 time-correlated single-photon counter at 20.0 ± 0.1 °C. Samples were excited at 331 nm, and the decays were deconvoluted from the instrument response function.[8,9]

Stopped-flow experiments were performed with a Bio-Sequential DX-17MV spectrofluorimeter from Applied Photophysics. Data acquisition and analysis were done using the

10.1021/jp035544c CCC: $25.00
Published on Web 09/30/2003

SX.18 software from Applied Photophysics. Solutions were mixed in a 1:1 ratio (10-mL syringes), and all measurements were performed at 20.0 ± 0.8 °C. Solutions were kept for 10 min in the thermostated housing to ensure that the temperature was equilibrated. The samples were excited with a 150 W Xe-arc lamp at 331 nm. The entrance and exit slits were set to a bandpass between 2.3 and 4.7 nm for the excitation monochromator. Fluorescence was detected at 90° to the excitation beam. The collected spectral region was selected using a cutoff filter at 455 nm (GG 455) for the pyrene excimer emission and an interference filter at 404 nm (fwhm of 38 nm, Melles Griot, lot 13637 (ANDV7248)) for the monomer emission. The PMT voltage was set for each experiment by optimizing the emission for the solution with the most intense fluorescence. An offset (3−4 V) was used to bring the initial intensity to zero and to maximize the dynamic range for the intensity changes (0.1−1.5 V). The stopped-flow traces contained 1000 points and up to 10 runs were averaged. The changes in the fluorescence intensities (I) were analyzed (SX.18 MV software) for the sum of exponentials (eq 1), where a_i, k_i, and b correspond to the amplitude change, the relaxation rate constant, and the intensity endpoint, respectively.

$$I = (\sum_{1}^{i} a_i \, e^{(-k_i t)}) + b \qquad (1)$$

Results and Discussion

Thermodynamics of Complexation. The complexation of pyrene to β-CD and γ-CD has been extensively studied.[10,11] In the case of β-CD, complexes with 1:1 and 1:2 (pyrene/CD) stoichiometries are formed.[12−15] Conflicting reports exist as to the stoichiometry and equilibrium constants for the complexes between pyrene and γ-CD.[16−18] A knowledge of the concentration of the different pyrene−γ-CD species is essential to the interpretation of the kinetic experiments. We studied the thermodynamics of complexation using steady-state and time-resolved fluorescence experiments combined with quenching studies. Our results are consistent with the stoichiometries (eqs 2−4) and equilibrium constants reported by Hamai.[18] Because our experiments basically confirm the results of a previous report, we presents details of the thermodynamic characterization in the Supporting Information, and only a brief description relevant to the kinetic studies is provided below.

$$\mathrm{Py} + \mathrm{CD} \overset{K_{11}}{\rightleftharpoons} \mathrm{PyCD} \qquad (2)$$

$$\mathrm{PyCD} + \mathrm{CD} \overset{K_{12}}{\rightleftharpoons} \mathrm{PyCD_2} \qquad (3)$$

$$\mathrm{PyCD} + \mathrm{PyCD} \overset{K_{22}}{\rightleftharpoons} \mathrm{Py_2CD_2} \qquad (4)$$

The pyrene monomer emission shows vibronic structure, and the ratio for the I (371 nm) to III (383 nm) bands is sensitive to the solvent polarity. This property has been extensively used to characterize the environment of pyrene when included in microheterogeneous systems.[19−22] In addition, singlet excited pyrene in the presence of ground-state pyrene forms an excimer, which shows a broad emission that is red-shifted from the monomer emission.

In the presence of γ-CD, the monomer and the excimer emissions of pyrene were observed (Figure 1). The excimer emission was assigned to the emission of the pyrene dimer in the 2:2 (pyrene/CD) complex. The ratio for the excimer emission intensity to the monomer intensity increased in the presence of γ-CD but decreased when the CD concentration was raised above 5 mM (inset of Figure 1). This result is consistent with the formation of a CD complex containing monomeric pyrene at high γ-CD concentrations, which corresponds to the formation of the 1:2 complex. The assignment of the excimer emission to the 2:2 complex is supported by a lack of growth for the excimer emission with time, a shift in the excitation spectrum when compared to that for the monomer emission, and a lower quenching efficiency of the excimer emission by iodide in the presence of γ-CD when compared to the efficiency in homogeneous solution.[8] The involvement of two CD molecules in the complex was confirmed by the disappearance of the excimer emission when the pH was raised above the pK_a of γ-CD (pK_a = 12.08).[23]

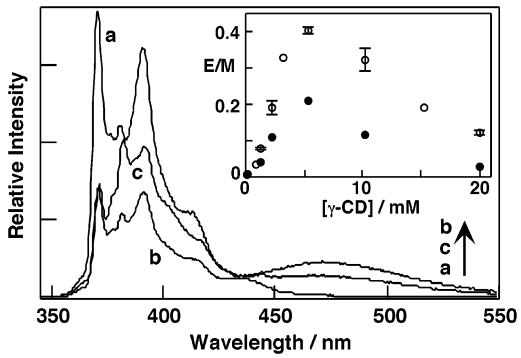

Figure 1. Corrected fluorescence spectra (λ_{ex} = 331 nm) for pyrene (0.5 μM) in (a) water and in the presence of (b) 5 mM and (c) 20 mM γ-CD. The inset shows the dependence of the intensity ratio for the excimer (473 nm) and monomer (383 nm) (E/M) emissions for 0.5 μM (○) and 0.25 μM (●) pyrene on the γ-CD concentration. The error bars correspond to the average deviation of two trials. Error bars smaller than the symbols are not shown.

In water, the pyrene monomer emission had a high I/III emission-intensity ratio (1.64 ± 0.02) (Figure 1). With increasing γ-CD concentrations, the monomer emission intensities as well as the I/III ratios changed. At each CD concentration, the pyrene monomer spectrum corresponds to the sum of the emission for each pyrene monomer species (i.e., free in water and bound as 1:1 or 1:2 CD complexes), taking into account their relative concentrations. At intermediate γ-CD concentrations (5 mM, Figure 1), the monomer intensity was lowest and a moderate decrease was observed for the I/III ratio (1.29 ± 0.05), whereas at high CD concentrations (20 mM, Figure 1) the monomer emission was raised and the I/III ratio decreased significantly (0.71 ± 0.01). The latter value is close to the ratio observed for pyrene emission in nonpolar solvents such as cyclohexane (0.58−0.60).[19,20] Steady-state and time-resolved quenching experiments with iodide were performed in the presence of 2 and 10 mM γ-CD.[8] Iodide resides primarily in the aqueous phase. A decrease in the monomer quenching efficiency signifies the protection of the pyrene inside the CD complex. Different singlet excited-state lifetimes were observed for pyrene in water and when complexed in the 1:1 and 1:2 (pyrene/CD) complexes. A decrease by a factor of 5 was observed for the quenching efficiency of the pyrene in the 1:1 complex, whereas the decrease was much larger for the 2:2 complex. The quenching results indicated that in the presence of 2 mM γ-CD most of the complexed monomeric pyrene was in the form of a 1:1 complex, whereas at high CD concentrations the 1:2 complex was present in a significant amount.

Determination of the Equilibrium Constants for the Pyrene−γ-CD Complexes. The excimer emission intensity is proportional to the concentration of the 2:2 complex and the

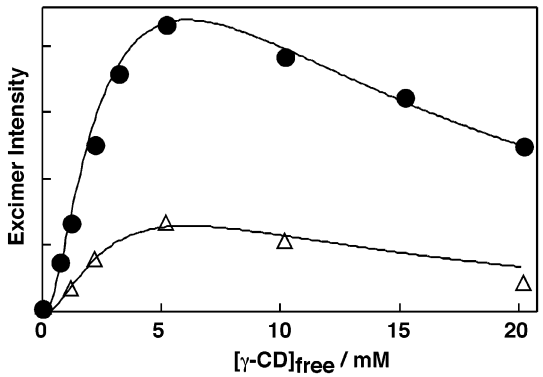

Figure 2. Numerical fit (—) to the change in excimer intensity with the γ-CD concentration, fitted simultaneously for the total concentrations of pyrene of 0.5 μM (●) and 0.25 μM (△) ($K_{11} = 280$ M^{-1}, $K_{12} = 100$ M^{-1}, and $K_{22} = 1.3 \times 10^6$ M^{-1}).

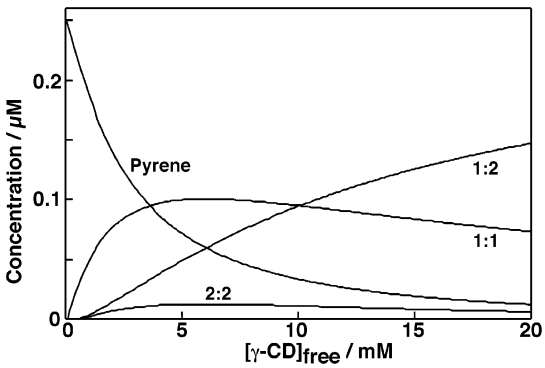

Figure 3. Dependence of the calculated concentrations of pyrene species ([pyrene]$_{total} = 0.25$ μM) on the concentration of free γ-CD.

emission quantum yield for the excimer. The variation in the excimer intensity with the γ-CD concentration was determined for pyrene concentrations of 0.5 and 0.25 μM (Figure 2). The intensities at both pyrene concentrations were simultaneously fitted numerically using the fitting routine in Scientist (Micromath v.2.02) (Figure 2). The expressions for the equilibrium constants, defined by eqs 2−4, and the mass balance equations for pyrene and cyclodextrins were used for the numerical fitting.[24] When all equilibrium constants (K_{11}, K_{12}, and K_{22}) were left as floating parameters, the recovered values had large statistical errors. For this reason, several fits were performed by fixing the parameter K_{11}. Acceptable fits based on statistical parameters, such as the squared correlation coefficient and the coefficient of determination, were obtained for K_{11} values between 240 and 320 M^{-1}. In addition, for K_{11} values outside this range systematic deviations from the experimental data points were observed. The K_{12} and K_{22} values recovered for the K_{11} range stated above were respectively 114 to 87 M^{-1} and 1.3×10^6 to 1.4×10^6 M^{-1}. Although the range recovered for the K_{22} values was narrow, the errors associated with this parameter for each individual fit were much larger. The equilibrium-constant values used for the calculation of the concentration of the pyrene−γ-CD species present in the dynamics studies were 280 ± 40 M^{-1} for K_{11}, 100 ± 14 M^{-1} for K_{12}, and $(1.3 \pm 0.5) \times 10^6$ M^{-1} for K_{22}. These values are similar to those reported previously by Hamai ($K_{11} = 300$ M^{-1}, $K_{12} = 170$ M^{-1}, $K_{22} = 1.3 \times 10^6$ M^{-1}).[18]

The concentration of free pyrene decreased continuously as the γ-CD concentration increased, whereas the concentrations of the 1:1 and 2:2 complexes were at a maximum at intermediate γ-CD concentrations (Figure 3). The concentration for the 1:2 complex was smaller than that of the 1:1 at low γ-CD concentrations, but the 1:2 complex dominated at high host concentrations (>10 mM).

Complexation Dynamics. The dynamics of pyrene complexation to γ-CD was studied using the stopped-flow technique, where two solutions were rapidly mixed (≤1.5 ms) and the relaxation processes toward an equilibrium were followed over time. Changes in the excimer or monomer emission intensities were measured. The changes in the excimer and monomer intensities are coupled for the equilibria shown in eqs 2−4 (i.e., when the monomer intensity increases, one expects the excimer intensity to decrease and vice versa). Changes in the concentration of the 2:2 complex were measured by monitoring the excimer emission intensity above 455 nm, and the monomer emission intensities were measured at 404 nm. From steady-state fluorescence experiments,[8] it was determined that the excitation spectrum for the excimer emission was broader than for the monomer emission. Excitation at 331 nm led to the excitation of the pyrene as a monomer and the pyrene dimer in the 2:2 complex, whereas for an excitation wavelength of 350 nm only the dimer in the 2:2 complex was excited. The molar absorptivity coefficients and fluorescence quantum yields for pyrene in water and in each CD complex are different. The samples were continuously irradiated during the stopped-flow experiment, and changes in the fluorescence intensity with time were measured. These fluorescence intensity changes were related to changes in the concentrations of free and CD-bound pyrene. This relationship is valid if one assumes that the molar absorptivity coefficients and fluorescence quantum yields for each pyrene−γ-CD species do not change with time. This assumption predicts that normalized kinetic traces for each mixing experiment should be the same when measured for different excitation wavelengths and when recording the monomer or excimer emissions (taking into account the inverse sign). The different molar absorptivity coefficients and fluorescence quantum yields have an effect on the amplitude of the signal, but do not have an effect on the recovered rate constants.

Several relaxation processes were observed over different time scales. The shortest relaxation process was complete within 200 ms (Figure 4). Three different mixing scenarios were employed, where solutions were mixed in a 1:1 ratio. (i) A decrease in the excimer emission was observed when the contents of one syringe containing a solution with both pyrene and γ-CD was mixed with the contents of a second syringe containing water (Figure 4A). In this case, the concentrations of pyrene and CD were halved within the dead time of the stopped flow, and the relaxation kinetics corresponds to a net decrease in 2:2 concentrations at the lower γ-CD concentrations. The effect is more pronounced for the lower γ-CD concentrations where the dependence of the 2:2 concentration on the CD concentration is more pronounced. (ii) An increase in the excimer emission intensity was observed when a solution containing pyrene was mixed with a second solution containing γ-CD ([γ-CD]$_{final} \leq$ 5 mM, Figure 4B). For this mixing scenario, there were no CD complexes formed before the solutions were mixed. The amplitude of the relaxation process increased as the concentration of γ-CD was increased. (iii) An increase in the 2:2 concentration was observed when a solution containing pyrene and γ-CD at a concentration greater than 2 mM was mixed with a solution containing pyrene at the same concentration as in the first syringe (Figure 4C). In this case, the pyrene concentration was kept constant, and the γ-CD concentration was halved during the mixing. The increase in the excimer emission intensity is related to the fact that once the solutions are mixed the initial 2:2 concentration is half of that in the syringe (arrow

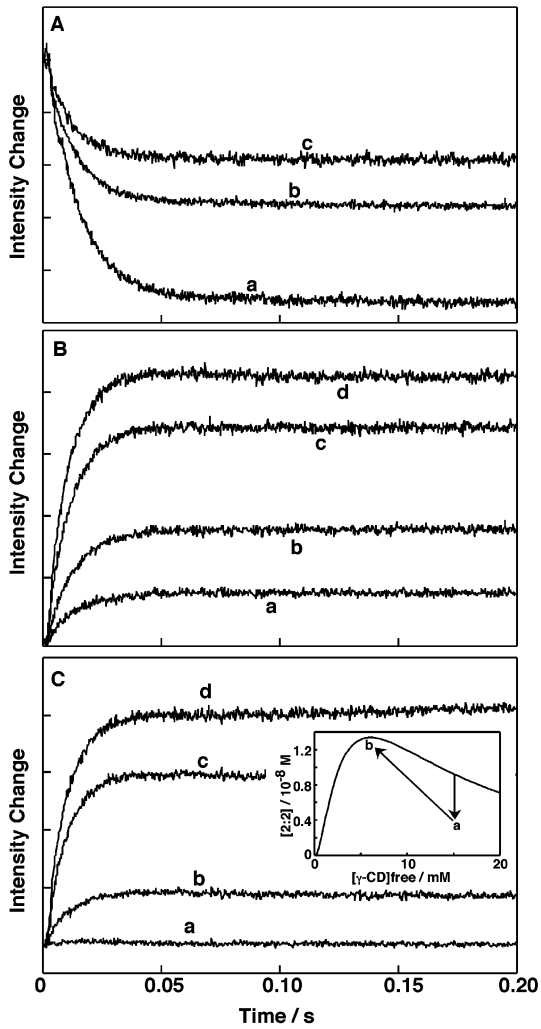

Figure 4. Changes in the excimer emission intensities measured in the stopped-flow experiment for different mixing scenarios in a 1:1 ratio. (A) Mixing of a solution containing pyrene ($[\text{pyrene}]_{\text{final}} = 0.25$ μM) and γ-CD ($[\gamma\text{-CD}]_{\text{final}}$: (a) 0.5 mM, (b) 1 mM, (c) 2.5 mM) in one syringe with water in the second syringe. (B) Mixing of a solution containing pyrene ($[\text{pyene}]_{\text{final}} = 0.25$ μM) with a solution containing γ-CD ($[\gamma\text{-CD}]_{\text{final}}$: (a) 0.5 mM, (b) 1 mM, (c) 2.5 mM, (d) 5 mM). (C) Mixing of a solution containing pyrene ($[\text{pyrene}]_{\text{final}} = 0.25$ μM) and γ-CD ($[\gamma\text{-CD}]_{\text{final}}$: (a) 0.5 mM, (b) 1 mM, (c) 2.5 mM, (d) 5 mM) with a solution containing only pyrene ($[\text{pyrene}]_{\text{final}} = 0.25$ μM). The inset shows the variation of the 2:2 concentration during the stopped-flow experiment. The arrow to point *a* corresponds to the instantaneous decrease in the concentration of the 2:2 complex by half when a solution containing pyrene and γ-CD was mixed with a solution containing only pyrene. The arrow from *a* to *b* corresponds to the re-equilibration process measured in the stopped-flow experiment.

leading to "a" in the inset of Figure 4C). The system then proceeds toward equilibrium (arrow leading to "b" in the inset of Figure 4C), and the excimer intensity increases. The same trends in the kinetics and observed rate constants were observed when the samples were excited at 331 or 350 nm. The changes in the monomer emission intensities were always in the opposite direction from the change in intensity observed for the excimer emission, but the recovered rate constants were the same. This result is consistent with the coupling of the processes leading to changes in the concentrations of free pyrene, 1:1 and 1:2 with changes in the 2:2 concentrations.

No CD complexes were initially present for the mixing of two solutions separately containing pyrene and γ-CD. For this reason, the first complex that formed was the 1:1 complex. The

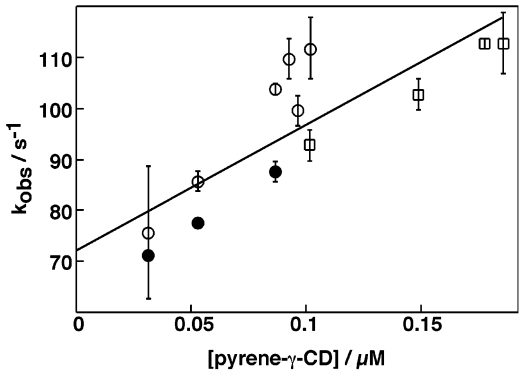

Figure 5. Dependence of the observed rate constant for the change in the excimer emission intensity on the final concentration of the 1:1 pyrene−γ-CD complex. The open symbols correspond to the mixing of a solution containing pyrene ($[\text{pyrene}]_{\text{final}}$: ○, 0.25 μM; □, 0.5 μM) with a solution containing γ-CD. The closed circles correspond to the mixing of water with a solution containing pyrene ($[\text{pyrene}]_{\text{final}} = 0.25$ μM) and γ-CD. The concentrations for the 1:1 complex were calculated using $K_{11} = 280$ M^{-1}, $K_{12} = 100$ M^{-1}, and $K_{22} = 1.3 \times 10^6$ M^{-1}.

2:2 complex was then formed from the association of two 1:1 complexes (eq 5). After mixing, the kinetics proceeded immediately to a decay of the monomer emission. This result showed that the formation of the 1:1 complex occurred within the mixing time of the stopped flow (<1.5 ms). This was expected on the basis of the fact that the complexation dynamics of other 1:1 CD complexes with guest molecules the size of the CD cavity occurs in the microsecond time domain.[25−34]

$$\text{PyCD} + \text{PyCD} \underset{k_-^{22}}{\overset{k_+^{22}}{\rightleftharpoons}} \text{Py}_2\text{CD}_2 \qquad (5)$$

For all mixing scenarios described, the kinetics followed a monoexponential function. The formation of the 2:2 complex is related to the association (k_+^{22}) and dissociation (k_-^{22}) rate constants (eq 5), and the change in the 2:2 concentration is given by eq 6:[35,36]

$$-\frac{\mathrm{d}[2:2]}{\mathrm{d}t} = (4k_+^{22}[1:1]_{\text{final}} + k_-^{22})[2:2] + 2k_+^{22}[2:2]^2 \qquad (6)$$

The second term in eq 6 can be neglected when the perturbation of the system is small[35] (i.e., the change in the concentration of the 2:2 complex is small when compared to the total 1:1 concentration). In this case, the kinetics follows a monoexponential function, and the observed relaxation rate constant is given by

$$k_{\text{obs}} = 4k_+^{22}[1:1]_{\text{final}} + k_-^{22} \qquad (7)$$

The concentration of the 1:1 complex for each pyrene and γ-CD concentration was calculated using the equilibrium constants determined from the fluorescence experiments. At each final concentration of the 1:1 complex, similar k_{obs} values were obtained, regardless of the mixing scenario employed. This result shows that the assumption made for the derivation of eq 7 (i.e., that the perturbation of the system was small) held even for the scenario where no CD complex was present prior to mixing. A linear relationship was observed for the dependence of k_{obs} on the final 1:1 concentration (Figure 5). The recovered values for k_+^{22} and k_-^{22} (eq 7) were respectively $(6.3 \pm 1.3) \times 10^7$ M^{-1} s^{-1} and 73 ± 5 s^{-1}. The ratio of these two rate constants corresponds to the equilibrium constants for the 2:2 complex ($K_{22} = k_+^{22}/k_-^{22}$). The value recovered from the kinetic studies ($(0.9 \pm 0.2) \times 10^6$ M^{-1}) is in agreement, within experimental

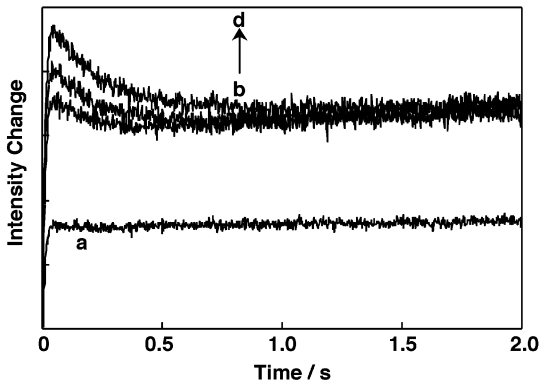

Figure 6. Changes in the excimer emission intensities measured in the stopped-flow experiment when a solution containing pyrene ($[\text{pyrene}]_{\text{final}} = 0.25\ \mu\text{M}$) was mixed in a 1:1 ratio with a solution containing γ-CD ($[\gamma\text{-CD}]_{\text{final}}$: (a) 5 mM, (b) 10 mM, (c) 15 mM, (d) 20 mM).

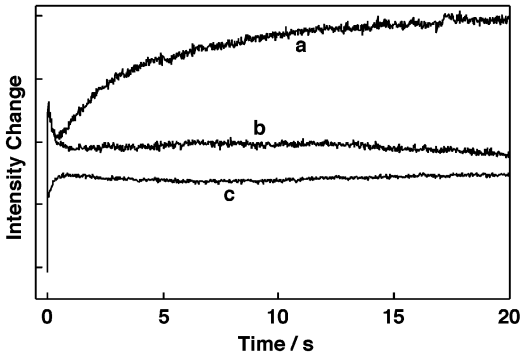

Figure 7. Changes in the excimer (a, b) and monomer (c) emission intensities measured in the stopped-flow experiment for the excitation of pyrene at 331 nm (a, c) or 350 nm (b) when a solution containing pyrene ($[\text{pyrene}]_{\text{final}} = 0.25\ \mu\text{M}$) was mixed with a solution containing γ-CD ($[\gamma\text{-CD}]_{\text{final}} = 10$ mM). The kinetic traces for the excimer emission were normalized at the maximum observed before 1 s.

error, with the value determined from the thermodynamic measurements ($(1.3 \pm 0.5) \times 10^6\ \text{M}^{-1}$). This agreement shows that the monitored relaxation process indeed corresponds to the formation of the 2:2 complex from the association of two 1:1 complexes.

The relaxation kinetics was also measured in D_2O for a mixing scenario where pyrene and γ-CD were contained in separate syringes. The observed rate constants for the complexation dynamics of the 2:2 complex were smaller in D_2O than in water. For example, the k_{obs} values for final concentrations of pyrene and γ-CD of 0.25 μM and 10 mM were $117 \pm 5\ \text{s}^{-1}$ in water compared to $70 \pm 4\ \text{s}^{-1}$ for the reaction in D_2O. This result suggests that the formation or cleavage of hydrogen bonds is involved in the complexation dynamics of the 2:2 complex. However, a quantitative evaluation was not possible because the thermodynamics of the pyrene complexation to γ-CD in D_2O would have to be known in order to calculate the final concentrations for the 1:1 complex.

For final γ-CD concentrations below 5 mM, the only observed relaxation process was the formation of the 2:2 complex. The monomer and excimer emission intensities were constant over periods of time longer than 200 ms. However, at higher γ-CD concentrations, a second relaxation process was observed that corresponded to a decrease in the excimer emission after the initial growth (Figure 6). This decrease was complete within 500 ms to 1 s. When the monomer emission was monitored, an increase in the emission intensity was observed for the second relaxation process, showing that the kinetics of the pyrene monomers and excimer were coupled. The amplitude for the second relaxation process increased as the γ-CD concentration was raised. The rate constant for this process was obtained by fitting the kinetic trace collected over 500 ms to the sum of two exponentials and the kinetic traces measured for 2 or 5 s to the sum of three exponentials. The observed rate constant for the second process did not change significantly within the experimental error ($4.5 \pm 1.5\ \text{s}^{-1}$) for different final γ-CD concentrations (7.5−20 mM) or different final pyrene concentrations (0.13−0.5 μM). When the experiments were performed in D_2O, no changes could be detected, within experimental error, for the observed rate constants. Finally, when the excimer emission intensity was normalized to its maximum within the first 100 ms, the amplitude for the second relaxation process was the same when the samples were excited at 331 or 350 nm. This control experiment is important because there was always a small contribution of monomer emission in the excimer detection region for samples excited at 331 nm.[37] The fact that the normalized amplitudes are the same for the different excitation wavelengths showed that only changes in the 2:2 concentration were monitored.

SCHEME 1

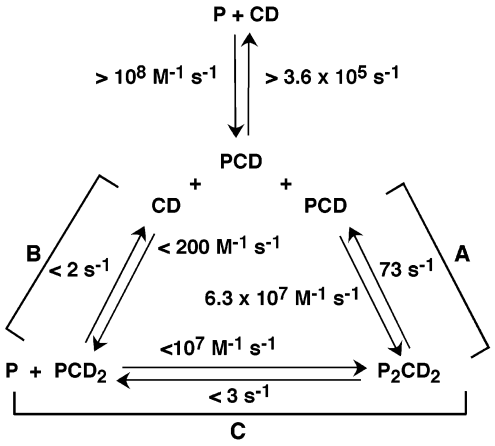

A third relaxation phase was observed after the decay of the excimer emission within 1 s. The kinetics for the excimer emission were very dependent on the excitation wavelengths (Figure 7). No changes were observed for excitation at 350 nm, but substantial changes were seen when pyrene was excited at 331 nm. In addition, the changes in the excimer and monomer emission intensities were not coupled. These effects were more prominent at intermediate γ-CD concentrations ($[\gamma\text{-CD}]_{\text{final}} =$ 7.5−10 mM) but were also present at higher CD concentrations. The rate constant for the third relaxation process could be reliably measured only for reasonably large amplitudes. No discernible trends were observed with the CD or pyrene concentrations. The average value for k_{obs} was $(0.4 \pm 0.1)\ \text{s}^{-1}$. No deuterium isotope effect was detectable within the experimental error.

Model for the Complexation Dynamics of Pyrene with γ-CD. From the thermodynamic measurements, it was determined that three pyrene−γ-CD complexes are formed. The possible reactions leading to these complexes are shown in Scheme 1. Full equilibration requires a maximum of three relaxation processes because one of the branches A, B, or C in Scheme 1 is redundant. The species leading to monomer (free pyrene, 1:1 and 1:2 complexes) and excimer (2:2 complex) emission are coupled by the equilibria shown in Scheme 1. Therefore, it is a necessary condition that the kinetics measured for the monomer and excimer emission be coupled. Three

different relaxation processes were observed for the kinetics of pyrene complexation with γ-CD. The observed rate constants for these three relaxation processes differ by at least 1 order of magnitude, and as a first approximation, the kinetics for each relaxation phase can be treated separately.

The formation of the 1:1 pyrene−γ-CD complex corresponds to one of the three expected relaxation processes for the model in Scheme 1. This relaxation process is fast and it is finished within the mixing time of the stopped flow. Of the three relaxation processed observed after mixing, the first two showed coupled kinetics, whereas for the slowest one the kinetics for the monomer and excimer emission were uncoupled. The uncoupled kinetics suggests that this relaxation process is not due to the formation of a complex with a stoichiometry different from those shown in Scheme 1. A possible explanation for the slow relaxation process is the slow internal rearrangement of one of the complexes, which leads to a change in emission quantum yields of pyrene without changing the concentration of CD complexes. An example of such an rearrangement would be the expulsion of water from the interior of the CD cavity after the formation of the 1:2 complex, leading to an increase in the pyrene monomer singlet excited-state lifetime. It will be necessary to perform kinetic measurements at defined emission wavelengths so that the species responsible for the change in the emission intensities can be identified in order to explore why these uncoupled relaxation processes occur. Unfortunately, the capability for conducting such experiments is presently not available. It is important to note that regardless of the origin of the third relaxation process its lifetime was much longer than for the first two processes, which occur within the first second after mixing. For this reason, the kinetics for the first two processes can be discussed within the framework of the model presented in Scheme 1.

The formation of the 1:1 complex occurred within the time resolution of the stopped-flow experiment, and for this reason only estimates can be provided for the association and dissociation rate constants of this process (Scheme 1). The association rate constants for guest molecules that are smaller than the CD cavity are typically larger than 1×10^8 M^{-1} s^{-1}.[26−31,34] On the basis of the equilibrium constant for the 1:1 complex ($K_{11} = k_+^{11}/k_-^{11}$), the dissociation rate constant is estimated to be larger than 3.6×10^5 s^{-1}.

At all γ-CD concentrations, an increase in the excimer emission, and therefore in the 2:2 concentration, was observed within the first 200 ms. This relaxation process was assigned to the formation of the 2:2 complex from the association of two 1:1 complexes. This assignment is consistent with the fact that the value derived for K_{22} from the kinetic studies is the same as the value measured from thermodynamic experiments. At high γ-CD concentrations, a second relaxation process was observed where the excimer emission decreased and the monomer emission increased. At these CD concentrations, fluorescence experiments indicated that the pyrene monomer was mainly in a nonpolar environment. These results are consistent with a decrease in the 2:2 concentration and a concomitant increase in the 1:2 concentration. The formation of the 2:2 complex is essentially finished within 200 ms, and at high CD concentrations an accumulation of the 2:2 complex is seen in excess of that observed for the thermodynamic equilibrium because the formation of the 1:2 complex is slow. The fast formation of the 2:2 complex is followed by the slower re-equilibration, within 1 s, to the 1:2 complex. This re-equilibration can occur either by the loss of pyrene from the 2:2 complex (branch C, Scheme 1) or by the dissociation of the 2:2 complex into two 1:1 complexes and the interaction of a 1:1 complex with a free CD (branch B, Scheme 1). These two pathways can in principle be distinguished because a dependence on the γ-CD concentration was expected for the observed rate constant in the case of the formation of the 1:2 complex through branch B, whereas for branch C the rate constant is expected to vary with the pyrene concentration. Unfortunately, the large errors associated with the rate constant of the second relaxation process preclude this differentiation. However, the upper limits for the association and dissociation rate constants for each branch can be determined by assuming that only one of the branches is responsible for the formation of the 1:2 complex.

The observed relaxation rate constant for branch C in Scheme 1 is related to the association (k_+^C) rate constant of the 1:2 complex with pyrene free in solution, the dissociation rate constants (k_-^C) for pyrene exiting the 2:2 complex, and the final concentrations for free pyrene and the 1:2 complex (eq 8).[35,36]

$$k_{obs} = k_+^C([1{:}2]_{final} + [P]_{final}) + k_-^C \qquad (8)$$

For the limited range of final pyrene concentrations employed, the same value was observed for k_{obs} within experimental error (4.5 ± 1.5 s^{-1}). For the calculations of k_+^C and k_-^C, the average pyrene (0.25 μM) and CD concentrations (13 mM) were employed. The concentrations of free pyrene and the 1:2 complex were calculated using the equilibrium constants determined above, and these concentrations were respectively 0.025 and 0.116 μM. The equilibrium constant between the 1:2 and 2:2 complex (K_C) can be expressed as a function of the known equilibrium constants ($K_C = (K_{22}K_{11})/K_{12} = (3.6 \pm 1.6) \times 10^6$ M^{-1}). This equilibrium constant is equal to the ratio of the association and dissociation rate constants ($K_C = k_+^C/k_-^C$). The value for k_-^C (3 ± 2 s^{-1}) was calculated from eq 8 for the k_{obs} value of 4.5 ± 1.5 s^{-1}, and k_+^C (ca. 10^7) was determined from the values of K_C and k_-^C.

The second route for the formation of the 1:2 complex is through branch B. The formation of the 2:2 complex is fast and can be assumed to be in rapid equilibrium. The observed rate constants for the process in branch B are given by eq 9 because the concentration of free CD is always present in large excess over the concentration of the 1:1 complex:[35,36]

$$k_{obs} = k_+^{12}[CD] + k_-^{12} \qquad (9)$$

The value for k_-^{12} (2.0 ± 0.7 s^{-1}) was calculated from eq 9 for a CD concentration of 13 mM and by substituting $k_+^{12} = K_{12}\, k_-^{12}$ into the equation. The value for k_+^{12} was determined to be 200 ± 80 M^{-1} s^{-1}. It is worth noting that for these k_+^{12} and k_-^{12} values, the k_{obs} values calculated for γ-CD concentrations of 7.5 and 20 mM were respectively 3.5 and 6 s^{-1}. This range is within the lower and upper limits of the value determined for the relaxation rate constant (4.5 ± 1.5 s^{-1}), suggesting that the dependence of k_{obs} on the CD concentration would have been difficult to identify. As stated above, the values for k_+^{12} and k_-^{12} are upper limits because in the analysis that was performed we assume that the formation of the 1:2 complex occurs solely through branch B.

The dynamics for the pyrene−γ-CD complexes containing two CD molecules is much slower than the dynamics for the 1:1 complex. The upper limit for the exit of pyrene from the 2:2 complex ($k_-^C < 3$ s^{-1}) is much lower than the exit from the 1:1 complex ($k_-^{11} > 3.6 \times 10^5$ s^{-1}). This result suggests that pyrene enters the γ-CD cavity through the wider entrance

containing the secondary hydroxyl groups. In the 2:2 complex, the wider rims are facing each other and pyrene can exit only through the narrower entrance, leading to a marked decrease of the exit rate constant by at least 5 orders of magnitude. If the γ-CD molecules were interacting either through the narrower rims or through the interaction of one wide and one narrow rim, then the exit of pyrene would be expected to happen with the same rate constant as that estimated for the 1:1 complex. The dissociation of a filled or empty CD from a complex containing two γ-CD molecules is much slower than the dissociation of guest molecules from 1:1 complexes. This result suggests that in the dissociation processes for the complexes with more than one CD the solvation of the CD is important and slows down dissociation. The much slower dissociation for the 1:2 complex compared to that for the 2:2 complex can be explained by the higher energetic cost to solvate the empty CD cavity compared to the cost to solvate the pyrene$-\gamma$-CD 1:1 complex. This explanation is correct only if the water content in the 1:2 and 2:2 complexes inside the CD is smaller than for the 1:1 complexes. On the basis of the I/III emission-intensity ratio for monomeric pyrene, the polarity in the 1:2 complex is indeed much lower than in the 1:1 complex.

There is a significant difference, by a factor of at least 3×10^5, in the association rate constants of the 1:1 complex with an empty CD or with another 1:1 complex. This large difference is responsible for the observation of a transient excess of the 2:2 complex despite the large differential between the 1:1 (<0.1 μM) and the free γ-CD (>1 mM) concentrations. The association rate constant of two 1:1 complexes is somewhat lower than the diffusion-controlled limit for bimolecular reactions in water (6.5×10^9 M^{-1} s^{-1}).[38] This rate constant is high considering that the two CD molecules have to be aligned along an axis for the complex to be formed. The only difference between the reaction of a 1:1 complex with an empty CD and another 1:1 complex is that in the latter case the CD contains the guest. The 1:1 complex will contain less water to be removed from the interior of the cavity when compared to the empty CD. In addition, in the 1:1 complex the rim of the CD will be more rigid than in the empty CD, leading to a preorganization of the CD to an optimal geometry for interaction with another 1:1 complex. Molecular mechanics calculations suggested that CDs are flexible structures,[39] and the inclusion of a guest will make the rim of the CD rigid. This preorganization is akin to a template effect,[5,40] where the efficiency of the formation of a supramolecular system, in this case, the dimerization of γ-CD, is faster in the presence of a guest.

Consequences of the Slow Dynamics on the Function of CD Systems and for Supramolecular Systems in General. CDs are used as host systems to perform many different functions. Two examples are the use of CDs to stabilize drugs against their phototoxicity[41−44] and the application of CDs to achieve chiral separation in chromatography.[45,46] For the drug-stabilization function, it is important that the residence time of the drug inside the CD be long enough to inhibit unwanted interactions between the drug and biomolecules. The mixed results in using CDs as photostabilization agents could be related to a short residence time of the drug or reactive intermediates inside the CD cavity. The photostabilizing effect of CDs as drug carriers could be improved when using formulations that favor the formation of higher-order CD complexes. The slower dynamics of the complexes with two CDs when compared to that of 1:1 complexes could also be employed to optimize separation efficiencies when using CDs as separation agents in chromatography.

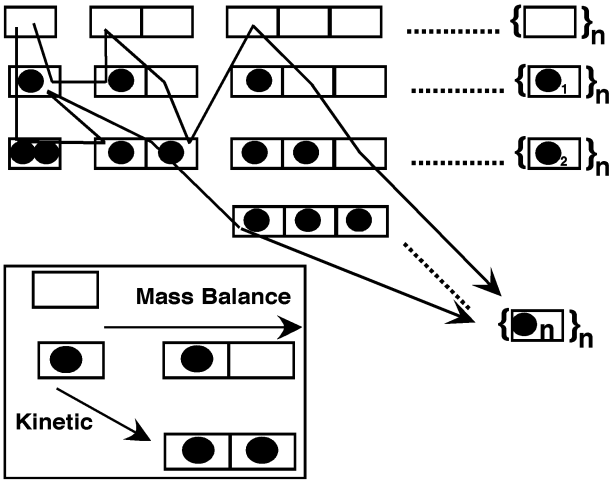

Figure 8. Schematic representation of a self-assembly matrix, where for each column the number of one component (squares) increases and for each row the number of the second component (circles) increases. The arrows show schematically two possible trajectories for the formation of an n/n complex. The expanded view corresponds to the part of the self-assembly matrix that describes the pyrene$-\gamma$-CD system.

In a more general sense, this work has impact when considering the kinetic control of structured assemblies. Kinetic control of self-assemblies has not yet been achieved by rational design. Self-assemblies are spontaneously formed by mixing several building blocks.[2,5,47] The stoichiometries of the various architectures can be manipulated by changing the initial relative concentrations of the building blocks because the final products are thermodynamic. From an abstract point of view, all of the possible structures for a self-assembly formed from two components can be expressed as a 2D matrix (Figure 8), where each column is related to an increased number of host molecules (squares) and each row corresponds to an increase in the number of guests (circles). After mixing the building blocks, we suggest that each growing structure explores a trajectory on the matrix until the thermodynamic product is formed. One of the conditions for self-assembly to occur is that the system has to undergo error corrections (i.e., trajectories not leading to the thermodynamic product have to be reversible). The physical basis for the formation of self-assemblies under thermodynamic control has been explored to establish the necessary conditions for self-assembly to occur.[48−50] The formation of structured assemblies under kinetic control has not been explored. The dynamics of the pyrene$-\gamma$-CD system showed that the transient enhancement of the kinetic (2:2 complex) product occurred on a time scale (hundreds of milliseconds) that is amenable to performing chemistry, as, for example, under continuous-flow conditions. The ability to form structures under kinetic control would provide access to a larger number of structures than available when considering only thermodynamic products, and one could conceivably work at mixtures of building blocks with very different concentration ratios. To explore the formation of structured assemblies under kinetic control, the dynamics of systems that contain components on at least two rows of the matrix (Figure 8) has to be investigated. This is the case for the pyrene$-\gamma$-CD system we studied, where the 1:2 complex is the thermodynamic product whereas the 2:2 complex is the kinetic product. The next steps toward kinetic control of structured assemblies is to establish the generality of the transient enhancement of host−guest systems with different stoichiometries, an understanding of how the competitive kinetic pathways can be manipulated, and proof of the concept that chemistry on a kinetically formed self-assembly is possible.

Acknowledgment. C.B. thanks the Natural Sciences and Engineering Research Council of Canada (NSERC) for the support of her research programs. A.S.M.D. thanks the NSERC for a PGSA scholarship, and U.K. thanks the NSERC for an USRA award and the RISE program for a RISE award. We thank Cerestar for the generous gift of γ-CD and L. Netter for continuous support in software development.

Supporting Information Available: A detailed description of the fluorescence studies to determine the stoichiometry of the pyrene−γ-CD complexes, the equations and definitions used for the numerical fitting in Scientist, and the derivations of the equations for the relaxation kinetics. This material is available free of charge via the Internet at http://pubs.acs.org.

References and Notes

(1) Lehn, J.-M.; Atwood, J. L.; Davies, J. E. D.; MacNicol, D. D.; Vögtle, F., Eds. *Comprehensive Supramolecular Chemistry*; Pergamon Press: New York, 1996.

(2) Lehn, J. M. *Supramolecular Chemistry: Concepts and Perspectives*; VCH: Weinheim, Germany, 1995.

(3) Balzani, V.; Gomez-Lopez, M.; Stoddart, J. F. *Acc. Chem. Res.* **1998**, *31*, 405−414.

(4) Gillard, R. E.; Raymo, F. M.; Stoddart, J. F. *Chem.—Eur. J.* **1997**, *3*, 1933−1940.

(5) Chapman, R. G.; Sherman, J. C. *Tetrahedron* **1997**, *53*, 15911−15945.

(6) Levin, M. D.; Stang, P. J. *J. Am. Chem Soc.* **2000**, *122*, 7428−7429.

(7) Kleinman, M. H.; Bohne, C. Use of Photophysical Probes to Study Dynamic Processes in Supramolecular Structures. In *Molecular and Supramolecular Photochemistry*; Ramamurthy, V., Schanze, K. S., Eds.; Marcel Dekker: New York, 1997; Vol. 1, pp 391−466.

(8) Details of the fluorescence experiments are provided in the Supporting Information.

(9) Bohne, C.; Redmond, R. W.; Scaiano, J. C. Use of Photophysical Techniques in the Study of Organized Assemblies. In *Photochemistry in Organized and Constrained Media*; Ramamurthy, V., Ed.; VCH Publishers: New York, 1991; pp 79−132.

(10) Rekharsky, M. V.; Inoue, Y. *Chem. Rev.* **1998**, *98*, 1875−1917.

(11) Bortolus, P.; Monti, S. *Adv. Photochem.* **1996**, *21*, 1−133.

(12) Kusumoto, Y. *Chem. Phys. Lett.* **1987**, *136*, 535−538.

(13) Muñoz de la Peña, A.; Ndou, T.; Zung, J. B.; Warner, I. M. *J. Phys. Chem.* **1991**, *95*, 3330−3334.

(14) Xu, W.; Demas, J. N.; DeGraff, B.; Whaley, M. *J. Phys. Chem.* **1993**, *97*, 6546−6554.

(15) Yang, H.; Bohne, C. *J. Phys. Chem.* **1996**, *100*, 14533−14539.

(16) Kobayashi, N.; Saito, R.; Hino, H.; Hino, Y.; Ueno, A.; Osa, T. *J. Chem. Soc., Perkin Trans. 2* **1983**, 1031−1035.

(17) Kano, K.; Takenoshita, I.; Ogawa, T. *Chem. Lett.* **1982**, 321−324.

(18) Hamai, S. *J. Phys. Chem.* **1989**, *93*, 6527−6529.

(19) Kalyanasundaram, K.; Thomas, J. K. *J. Am. Chem. Soc.* **1977**, *99*, 2039−2044.

(20) Dong, D. C.; Winnik, M. A. *Photochem. Photobiol.* **1982**, *35*, 17−21.

(21) Kalyanasundaram, K. *Photochemistry in Microheterogeneous Systems*; Academic Press: Orlando, FL, 1987.

(22) Ramamurthy, V. *Photochemistry in Organized and Constrained Media*; VCH Publishers: New York, 1991.

(23) Connors, K. A. *Chem. Rev.* **1997**, *97*, 1325−1357.

(24) The definition of the equations used for the numerical fitting routine in Scientist are given in the Supporting Information.

(25) Barra, M.; Bohne, C.; Scaiano, J. C. *J. Am. Chem. Soc.* **1990**, *112*, 8075−8079.

(26) Barra, M. *Supramol. Chem.* **1997**, *8*, 263−266.

(27) Barros, T. C.; Stefaniak, K.; Holzwarth, J. F.; Bohne, C. *J. Phys. Chem. A* **1998**, *102*, 5639−5651.

(28) Christoff, M.; Okano, L. T.; Bohne, C. *J. Photochem. Photobiol., A* **2000**, *134*, 169−176.

(29) Liao, Y.; Frank, J.; Holzwarth, J. F.; Bohne, C. *J. Chem. Soc., Chem. Commun.* **1995**, 199−200.

(30) Liao, Y.; Bohne, C. *J. Phys. Chem.* **1996**, *100*, 734−743.

(31) Okano, L. T.; Barros, T. C.; Chou, D. T. H.; Bennet, A. J.; Bohne, C. *J. Phys. Chem. B* **2001**, *105*, 2122−2128.

(32) Turro, N. J.; Okubo, T.; Chung, C.-J. *J. Am. Chem. Soc.* **1982**, *104*, 1789−1794.

(33) Turro, N. J.; Bolt, J. D.; Kuroda, Y.; Tabushi, I. *Photochem. Photobiol.* **1982**, *35*, 69−72.

(34) Nau, W. M.; Zhang, X. *J. Am. Chem. Soc.* **1999**, *121*, 8022−8032.

(35) Bernasconi, C. F. *Relaxation Kinetics*; Academic Press: New York, 1976.

(36) The derivations of the relaxation kinetics in general terms are shown in the Supporting Information.

(37) This small contribution of monomer emission was apparent in the time-resolved fluorescence experiments where the decay for the excimer emission follows the sum of two exponentials and where one of the lifetimes corresponds to that of pyrene in water. A decay of the monomer can also be observed in the excimer emission region when the fluorescence of pyrene in water is measured.

(38) Murov, S. L.; Carmichael, I.; Hug, G. L. *Handbook of Photochemistry*, 2nd ed.; Marcel Dekker: New York, 1993.

(39) Lipkowitz, K. B. *J. Org. Chem.* **1991**, *56*, 6357−6367.

(40) Busch, D. H.; Vance, A. L.; Kolchinski, G. Molecular Template Effect: Historical View, Principles, and Perspectives. In *Templating, Self-Assembly, and Self-Organization*; Sauvage, J.-P., Hosseini, M. W., Eds.; Comprehensive Supramolecular Chemistry; Atwood, J. L., Davies, J. E., MacNicol, D. D., Vögtle, F., Lehn, J.-M., Eds.; Elsevier Science Ltd.: New York, 1996; Vol. 9, pp 1−42.

(41) Hoshino, T.; Ishida, T.; Irie, T.; Hirayama, F.; Euekama, K.; Yamasaki, M. *J. Incl. Phenom.* **1988**, *6*, 415−423.

(42) De Guidi, G.; Condorelli, G.; Guifridda, S. P., G.; Giammoma, G. *J. Inclusion Phenom.* **1993**, *15*, 43−58.

(43) Condorelli, G.; De Guidi, G.; Giuffrida, S.; Costanzo, L. L. *Coord. Chem. Rev.* **1993**, *125*, 115−128.

(44) Monti, S.; Sortino, S. *Chem. Soc. Rev.* **2002**, *31*, 287−300.

(45) Li, S.; Purdy, W. C. *Chem. Rev.* **1992**, *92*, 1457−1470.

(46) Snopek, J.; Smolková-Keulemansová, E.; Cserháti, T.; Gahm, K. H.; Stalcup, A. Cyclodextrins in Analytical Separation Methods. In *Cyclodextrins*; Szejtli, J., Osa, T., Eds.; Comprehensive Supramolecular Chemistry; Atwood, J. L., Davies, J. E. D., MacNicol, D. D., Vögtle, F., Lehn, J.-M., Eds.; Pergamon Press: New York, 1996; Vol. 3, pp 515−572.

(47) Sauvage, J.-P.; Hosseini, M. W. Templating, Self-Assembly, and Self-Organization. In *Comprehensive Supramolecular Chemistry*; Atwood, J. L., Davies, J. E., MacNicol, D. D., Vögtle, F., Lehn, J.-M., Eds.; Elsevier Science Ltd.: New York, 1996; Vol. 9.

(48) D'Arceneo, C.; Doddi, G.; Ercolani, G.; Mencarelli, P. *Chem.—Eur. J.* **2000**, *6*, 3540−3546.

(49) Ercolani, G. *J. Phys. Chem. B* **1998**, *102*, 5699−5703.

(50) Ercolani, G. *J. Phys. Chem. B* **2003**, *107*, 5052−5057.